Distributed mode filtering rod fiber amplifier delivering 292W with improved mode stability.

Laurila, Marko; Jørgensen, Mette Marie; Hansen, Kristian Rymann; Alkeskjold, Thomas T.; Broeng, Jes; Lægsgaard, Jesper

Published in:
Optics Express

Link to article, DOI:
10.1364/OE.20.005742

Publication date:
2012

Document Version
Publisher's PDF, also known as Version of record

Distributed mode filtering rod fiber amplifier delivering 292W with improved mode stability

Marko Laurila, [1,*] Mette M. Jørgensen,[2] Kristian R. Hansen,[1] Thomas T. Alkeskjold,[2] Jes Broeng,[2] and Jesper Lægsgaard[1]

[1]*DTU Fotonik, Department of Photonics Engineering, Technical University of Denmark, 2800 Kgs. Lyngby, Denmark,*

[2]*NKT Photonics, Blokken 84, 3460 Birkerød, Denmark*

[*]*malau@fotonik.dtu.dk*

Abstract: We demonstrate a high power fiber (85μm core) amplifier delivering up to 292Watts of average output power using a mode-locked 30ps source at 1032nm. Utilizing a single mode distributed mode filter bandgap rod fiber, we demonstrate 44% power improvement before the threshold-like onset of mode instabilities by operating the rod fiber in a leaky waveguide regime. We investigate the guiding dynamics of the rod fiber and report a distinct bandgap blue-shifting as function of increased signal power level. Furthermore, we theoretically analyze the guiding dynamics of the DMF rod fiber and explain the bandgap blue-shifting with thermally induced refractive index change of the refractive index profile.

OCIS codes: (060.2320) Fiber optics amplifiers and oscillators; (060.4005) Micro structured fibers.

References and links

1. J. Limpert, O. Schmidt, J. Rothhardt, F. Röser, T. Schreiber, A. Tünnermann, S. Ermeneux, P. Yvernault, and F. Salin, "Extended single-mode photonic crystal fiber lasers," Opt. Express **14**(7), 2715–2720 (2006).
2. C. D. Brooks and F. D. Teodoro, "Multimegawatt peak-power, single-transverse-mode operation of a 100μm core diameter, Yb-doped rodlike photonic crystal fiber amplifier," Appl. Phys. Lett. **89**(11), 111119 (2006).
3. F. Jansen, F. Stutzki, H. J. Otto, M. Baumgartl, C. Jauregui, J. Limpert, and A. Tünnermann, "The influence of index-depressions in core-pumped Yb-doped large pitch fibers," Opt. Express **18**(26), 26834–26842 (2010).
4. T. T. Alkeskjold, M. Laurila, L. Scolari, and J. Broeng, "Single-Mode ytterbium-doped Large-Mode-Area photonic bandgap rod fiber amplifier," Opt. Express **19**(8), 7398–7409 (2011).
5. A. V. Smith and J. J. Smith, "Mode instability in high power fiber amplifiers," Opt. Express **19**(11), 10180–10192 (2011).
6. T. Eidam, C. Wirth, C. Jauregui, F. Stutzki, F. Jansen, H. J. Otto, O. Schmidt, T. Schreiber, J. Limpert, and A. Tünnermann, "Experimental observations of the threshold-like onset of mode instabilities in high power fiber amplifiers," Opt. Express **19**(14), 13218–13224 (2011).
7. C. Jauregui, T. Eidam, J. Limpert, and A. Tünnermann, "The impact of modal interference on the beam quality of high-power fiber amplifiers," Opt. Express **19**(4), 3258–3271 (2011).
8. K. R. Hansen, T. T. Alkeskjold, J. Broeng, and J. Lægsgaard, "Thermo-optical effects in high-power ytterbium-doped fiber amplifiers," Opt. Express **19**(24), 23965–23980 (2011).
9. F. Stutzki, F. Jansen, T. Eidam, A. Steinmetz, C. Jauregui, J. Limpert, and A. Tünnermann, "High average power large-pitch fiber amplifier with robust single-mode operation," Opt. Lett. **36**(5), 689–691 (2011).
10. M. Laurila, J. Saby, T. T. Alkeskjold, L. Scolari, B. Cocquelin, F. Salin, J. Broeng, and J. Lægsgaard, "Q-switching and efficient harmonic generation from a single-mode LMA photonic bandgap rod fiber laser," Opt. Express **19**(11), 10824–10833 (2011).
11. I. Manek-Hönninger, J. Boullet, T. Cardinal, F. Guillen, S. Ermeneux, M. Podgorski, R. Bello Doua, and F. Salin, "Photodarkening and photobleaching of an ytterbium-doped silica double-clad LMA fiber," Opt. Express **15**(4), 1606–1611 (2007).

1. Introduction

During the last years, photonic crystal based fiber lasers and amplifiers have undergone a massive improvement both with respect to beam quality performance and high average and peak power. High pulse energies and peak powers require large effective area and new fiber designs have been shown [1], delivering extreme pulse energies with close to diffraction limited beam operation [2]. However, large effective area fibers often support increasing

#160026 - $15.00 USD Received 14 Dec 2011; revised 16 Feb 2012; accepted 21 Feb 2012; published 24 Feb 2012

number of higher order modes and new methods to suppress them have been demonstrated [3,4]. Recently, experimental and theoretical studies have shown beam quality degradation of Large Mode Area (LMA) fiber lasers and amplifiers when operating at high average power levels [5–8]. This manifests as severe mode instabilities, occurring at some threshold level, which seems mostly to depend on the effective area and inversion profile [6]. The causes of the mode instabilities are still under discussion, and recent development has pushed the level for mode instabilities by using so-called Large-Pitch Fibers [9].

In this paper, we demonstrate the performance of a photonic bandgap rod fiber design having precisely tuned Distributed Mode Filtering (DMF) elements [4]. The same rod fiber design was used in a Q-switched laser configuration with high efficiency and good beam quality, without indication of mode instabilities [10]. However, in those experiments the output power was limited by available pump power and modal instabilities was not observed. In this paper/work, we use the same rod fiber design in an amplifier configuration with up to 600W of available pump power. We study the limits of the DMF fiber design and demonstrate a 44% power improvement before the threshold-like onset of mode instabilities by operating the rod fiber in an initial leaky waveguide regime. In addition, we study the guiding dynamics of the DMF rod fiber using a broadband amplifier configuration and demonstrate a clearly observed indicator of the refractive index profile change.

The paper is arranged as follows: in section 2 we shortly discuss the guiding dynamics of the DMF rod fibers. In section 3 we describe out amplifier experiments and observations. In section 4 we demonstrate a possible origin of the improved performance and in details study the guiding dynamics of the DMF rod fibers by experiments and simulations. In section 5 we conclude the work.

2. Guiding dynamics of the DMF rod fiber

The DMF rod fibers have different guiding regimes and are designed to work in a specific wavelength range [4, 10]. Figure 1(a) shows a transmission measurement of a passive DMF rod fiber, having a mode field diameter of 60μm, and measured Near Field (NF) images at two different guiding regimes, one at the leaky region (1030nm) and one at the Single Mode (SM) region (1060nm). The oscillations in the spectrum originate from modal interference of the guided modes of the rod fiber as they are coupled to the pick-up fiber. No oscillations are observed in the range 1050-1070nm which indicates that the Higher Order Modes (HOMs) are phase matched to the cladding modes and therefore only the Fundamental Mode (FM) is guided in the core. Oscillations are observed towards longer wavelengths, which indicate interference between the FM mode and HOMs in the core region. Leaky regimen corresponds to the region where the FM couples out to the cladding band [10].

#160026 - $15.00 USD Received 14 Dec 2011; revised 16 Feb 2012; accepted 21 Feb 2012; published 24 Feb 2012

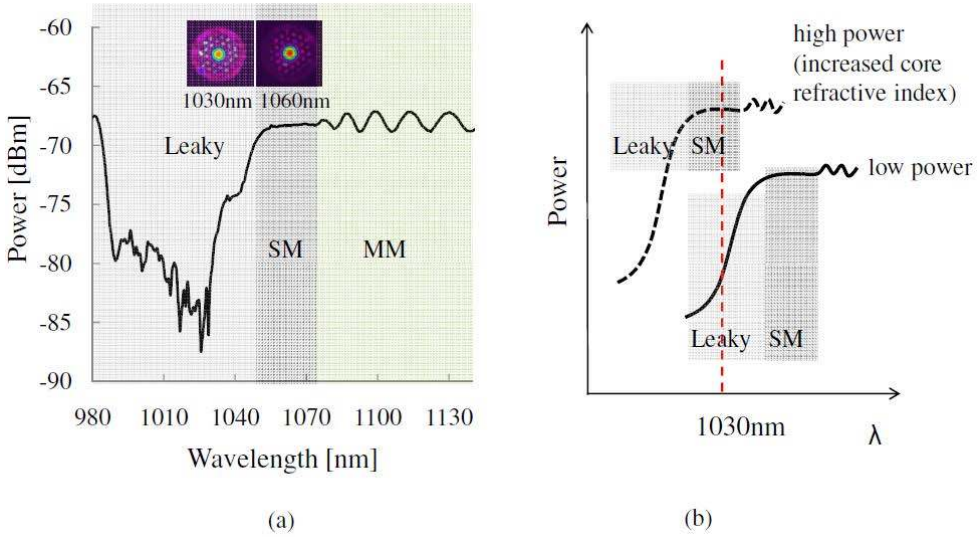

Fig. 1. (a) Transmission measured of a passive DMF rod fiber having a mode field diameter of 60µm. Interference patterns, in the spectrum indicate multimode behavior, a dip the leaky regime, and the single mode region can be identified between 1050nm – 1070nm. Measured near field images show the guiding dynamics of the DMF rod fiber. (b) Sketched illustration of the guiding regions movement at low and high power operation.

If the refractive index of the core is increased, the transmission spectrum in Fig. 1(a) will move towards the blue wavelengths. However, the DMF resonant elements in the cladding structure will move the transmission spectrum towards the red wavelength when their refractive index is increasing. In a case of an ytterbium doped DMF rod fiber, thermal load, which is mainly confined to the core, can cause the refractive index to increase, when the signal power is increasing, and if the DMF rod fiber is operated in a leaky wavelength regime, a certain thermal load move operation into SM region, illustrated in Fig. 1(b). A signal at 1030nm is firstly weakly confined to the core but after the DMF filtering blue shifting the signal becomes more confined to the core and therefore is at the SM guiding region. In section 3, we will study this behavior by operating two DMF rod fibers in different guiding regimes.

3. Experiments

We use a linearly polarized seed source delivering ~30ps pulses at 1032.2nm with 40MHz repetition rate, having a 10dB spectral width of 0.7nm (~0.3nm FWHM) at 1.1W of average output power, shown in Fig. 2, and max average output power of 19W. The rod fibers under test are pumped in counter-propagating direction with a pump module delivering up to 600W of pump power (976nm, 400µm, 0.22NA). We single-pass both the pump and the signal and use a CCD camera, at the output side, to verify the quality of the output beam (Spiricon GRAS20, frame rate ~20Hz). We use two different ytterbium-doped double-clad DMF rod fibers, which were manufactured to be single mode in two different wavelength regions, one at 1030-1045nm, referred to as “DMF1030” and the other at 1050-1070nm, referred to as “DMF1064”. The DMF rod fibers have a core diameter of ~85µm, an estimated core NA ~0.01 and a pump cladding of 265-270µm with ~0.6NA. The length of the DMF rod fibers is 90cm, having pump absorption of ~27dB/m (nominal) at 976nm. Both of the ends are prepared with AR-coated end caps.

#160026 - $15.00 USD Received 14 Dec 2011; revised 16 Feb 2012; accepted 21 Feb 2012; published 24 Feb 2012

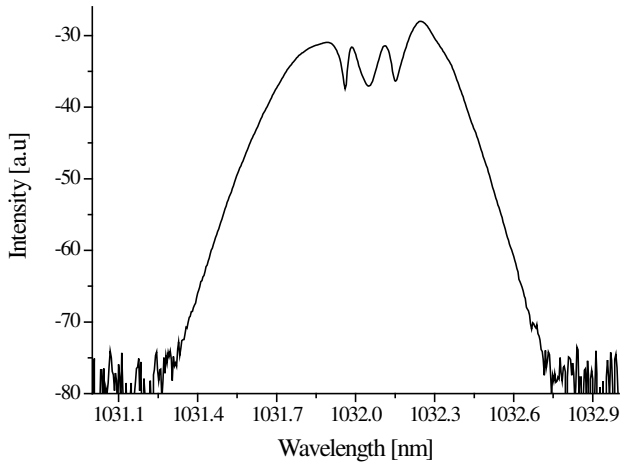

Fig. 2. Output spectrum of the seed source at 1.1W of average output power having a 10dB spectral width of 0.7nm (~0.3nm FWHM).

In the first test, we used a seed power of 1.1W (1032.2nm) and measured the slope efficiency up to the onset level of mode instabilities for the two DMF rod fibers, shown in Fig. 3. Both of the rod fibers have >70% slope efficiency but the threshold level of the mode instabilities is different.

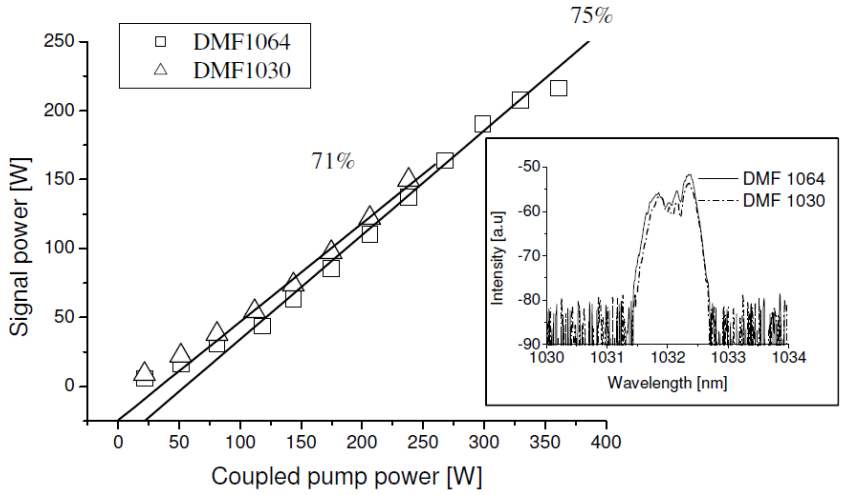

Fig. 3. Slope efficiency measurement of the DMF1030 and the DMF1064 and recorded output spectra at the maximum output powers.

At ~150W of output power the DMF1030 start to suffer from mode instabilities, shown in Fig. 4, but for the DMF1064 mode instabilities is observed at 216W. We applied the same method for evaluating the mode instabilities threshold level as in [6], a power level where the output beam quality shows a first sign of a temporal change, from single mode to a random temporal movement. This method requires a fast detection device to fully resolve the first temporal changes of the beam quality. The CCD camera used in the experiment had a frame rate of ~18Hz but still provides a repeatable way to compare different rod fiber samples with +/−10W repeatability. Spectral broadening of the amplified signal is small and the measured

#160026 - $15.00 USD Received 14 Dec 2011; revised 16 Feb 2012; accepted 21 Feb 2012; published 24 Feb 2012

output spectra have 10dB spectral width of ~0.9nm (FWHM ~0.3nm), shown in the inset of Fig. 3.

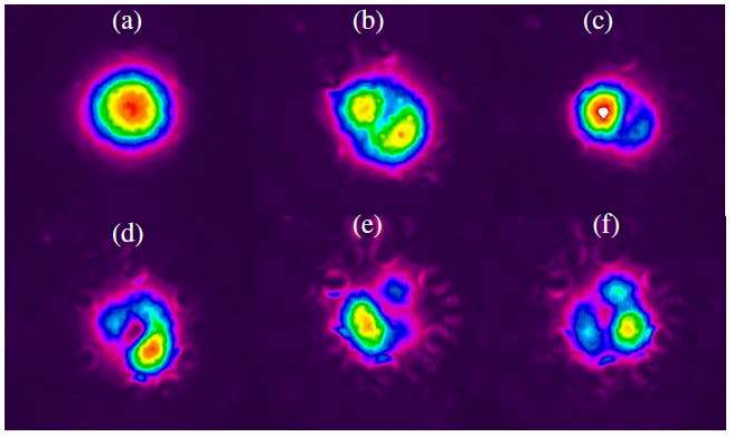

Fig. 4. Measured beam quality of the DMF1030 below and above the threshold-like onset of mode instabilities. (a) below (<150W) (b)-(f) above the threshold level (>155W).

When the DMF1064 is seeded with a 1032nm signal it operates in a leaky waveguide regime, where the fundamental mode is partly coupled to the DMF elements and has high confinement loss. At low output power levels (<50W), the core mode appears to be leaky with high amount of cladding light, but becomes more confined at higher output power levels (>80W), as shown in Fig. 5. This can also be observed from the signal core to cladding ratio measurement, shown in Fig. 5, which shows that the core light increases from 60% to 93% with increasing power. The increased confinement loss at low power levels also decreases the measured slope efficiency at low power levels, as shown in Fig. 3.

This indicates that the confinement loss decreases with increasing output power levels which could be caused by a thermally induced change in the refractive index profile. As the DMF1064 is operated in the leaky regime at low power levels and as the power is increased, the thermal load will raise the refractive index of the core and the DMF filtering effect is blue shifted. The guiding dynamics of the DMF rod fibers will be discussed more in section 4, where we will, in detail, analyze the index change.

#160026 - $15.00 USD Received 14 Dec 2011; revised 16 Feb 2012; accepted 21 Feb 2012; published 24 Feb 2012

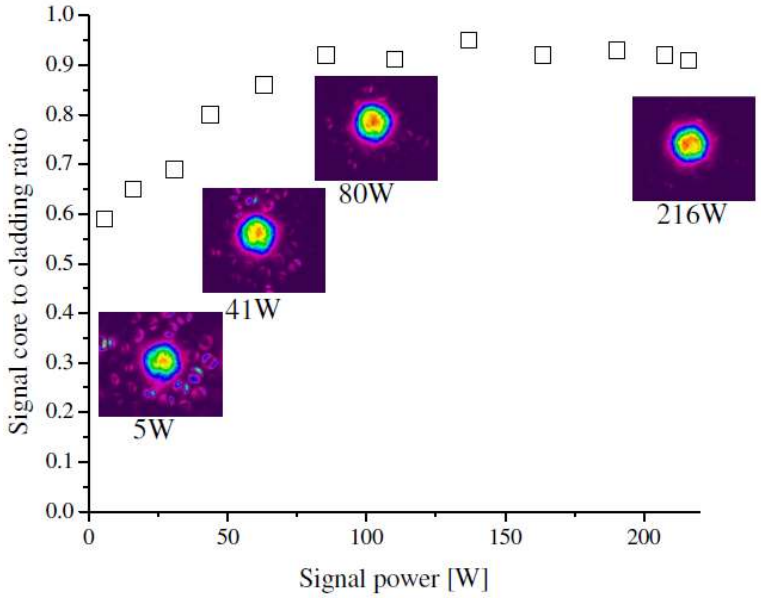

Fig. 5. Measured signal core to cladding ratio of the DMF1064 and recorded evolution of near-field image quality at different signal output powers (1032nm seed).

The DMF1030 is operated in the SM wavelength region in all the power levels and therefore the confinement loss is low. The measured signal core to cladding ratio, except at low power (<10W), is constant 90 – 97% and the mode appears to be nicely confined in the core, shown in Fig. 6.

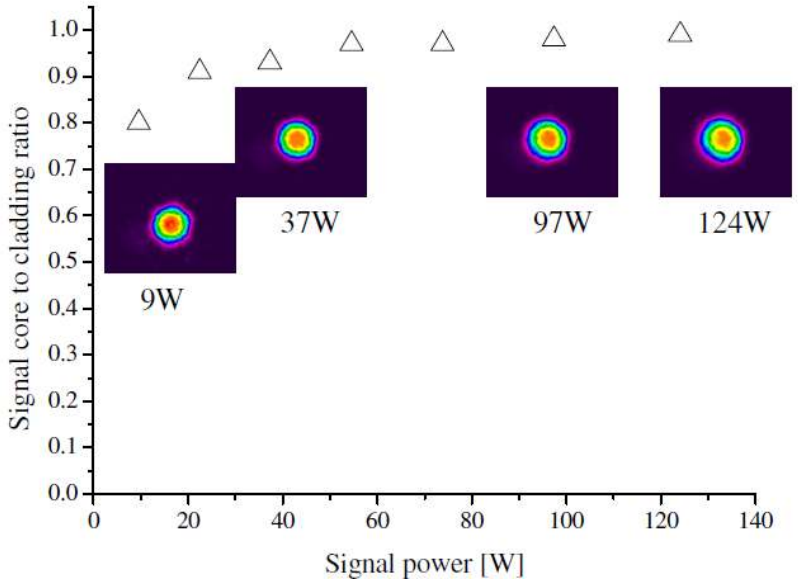

Fig. 6. Measured signal core to cladding ratio of the DMF1030 and recorded evolution of near-field image quality at different signal output powers (1032nm seed).

One possible cause of the mode instabilities is the formation of inversion and/or thermal Long-Period Grating (LPG) formed by the interference between the fundamental and higher

#160026 - $15.00 USD Received 14 Dec 2011; revised 16 Feb 2012; accepted 21 Feb 2012; published 24 Feb 2012

order modes [7], which can be supported by a single-mode waveguide under strong thermal load [8]. Gain and therefore inversion plays a vital role on the formation of this LPG and thereby gain dynamics will change the onset level of the mode instabilities [6]. In the second test, we used a DMF1064 rod fiber (101cm) in the same amplifier configuration but with much higher seed level, 15W. With this seed level, we could reach 292W of average output power level before the threshold-like onset of the mode instabilities.

As the experiment was repeated multiple times, we observed a decrease in the threshold-like onset of the mode instabilities. This indicates that the fiber possesses a memory effect, possibly because the LPG grating discussed above has a component which is of a permanent nature. A permanent inscription of index changes by high-power radiation could be related to the color-center formation commonly associated with photodarkening phenomena. We performed a set of measurements on the DMF1064 rod fiber, where we obtained the onset level of the mode instabilities ten times, while letting the system to cool down ~1min between each test and keeping the system above the threshold level roughly 10 sec before decreasing the pump power. The onset level of the mode instabilities was lowered from ~292W down to ~230W after few tests and stabilized around 230W. If the formation of the LPG is linked to color center formation, it can be, with some limitations, removed by bleaching either thermally or optically [11]. We therefore, exposed the rod fiber with blue irradiation (405nm, ~20mW) from a laser source. Light from the laser source was coupled into the inner cladding of the rod fiber and exposed for 20hours. After the photobleaching, the earlier test was repeated. The onset level of the mode instabilities recovered back to original level (~285W) but once again the onset level decreased when experiment was repeated, shown in Fig. 7. Error bars in the Fig. 7 shows inaccuracy caused by the slow detection system (± 10W). It seems that photobleaching can remove the formed LPG grating (or at least part of it) but, as shown [11], the photobleaching is reversible process and it will not prevent future formation of the LPG grating. Other means for photobleaching can also be imagined, such as bleaching simultaneously with laser operation, and/or using other wavelengths.

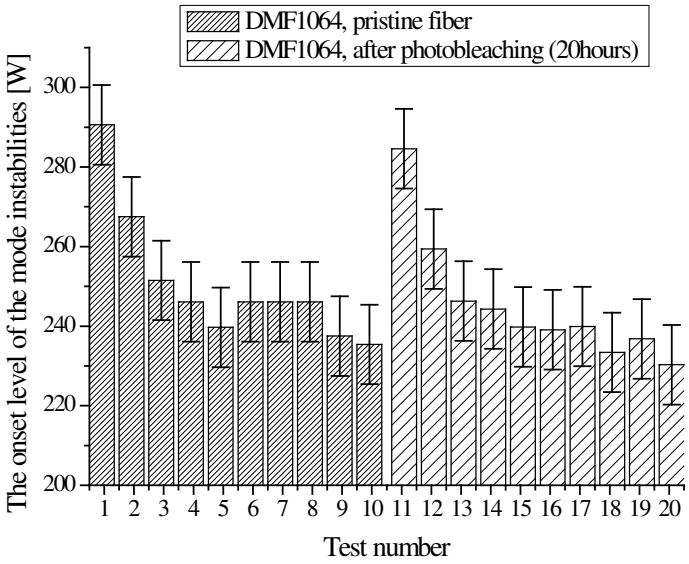

Fig. 7. Development of the mode instabilities onset level of a pristine rod fiber and after photobleaching it with blue laser source (405nm, 20mW, 20hours). Error bars ± 10W represent the inaccuracy caused by the slow detection system.

#160026 - $15.00 USD Received 14 Dec 2011; revised 16 Feb 2012; accepted 21 Feb 2012; published 24 Feb 2012

4. Experiments and simulations of guiding dynamics

We measured the edge of the bandgap movement of the DFM1064 rod fiber (101cm long) by seeding the rod fiber with an Amplified Spontaneous Emission (ASE) source (1.1W input) and varying the pump power. Figure 8 shows an input ASE signal spectrum and typically measured output spectrum of two rod fibers with similar parameters (core diameter, pump absorption, doping level), one without (reference rod fiber) and one with the DMF elements. The spectrum obtained from the rod fiber with DMF elements (DMF1064) shows clear edge of the bandgap, leaky wavelength regime at ~1040nm, while the output spectrum from the rod fiber without the DMF elements is smooth without any indication of bandgaps.

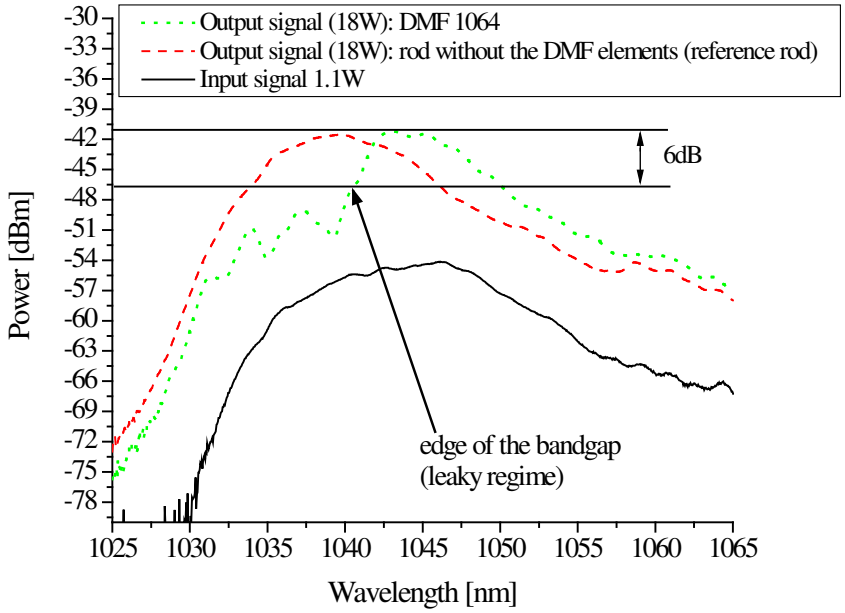

Fig. 8. Measured spectrum of the input ASE signal and output spectra of two different rod fibers, one without the DMF elements and one with the DMF elements (DMF1064) under same pumping conditions. The DMF1064 shows clearly resolved edge of the bandgap, leaky wavelength regime, at ~1040nm.

We measured the output spectrum at different signal power levels up to ~160W and used 6dB power criteria to identify the edge of the bandgap, as shown in Fig. 8. The measured output spectra were subtracted from the input spectrum and gain induced bandgap blueshift was corrected using a reference gain profile for each power level. The reference gain profiles were obtained from a reference rod fiber without the DMF elements. Without the gain correction, the measured bandgap position would be more blue shifted as increasing ytterbium gain peaking at 1030nm.

#160026 - $15.00 USD Received 14 Dec 2011; revised 16 Feb 2012; accepted 21 Feb 2012; published 24 Feb 2012

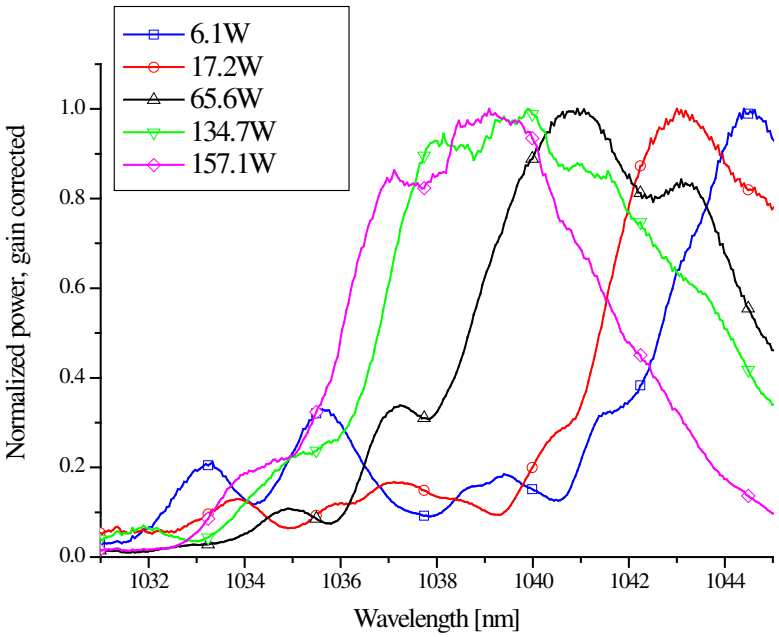

Fig. 9. Measured bandgap shift of the DMF1064 at different output power levels.

The movement of the bandgap is a clear evidence of the thermally induced refractive index profile change of the rod fiber. The thermal load is highest at the output end of the rod fiber declining towards the input end and thereby the bandgap blueshift is gradually along the whole fiber length. The measurement thereby shows the effective bandgap position not the absolute or local bandgap position as the edges of the bandgap are smeared. Figure 9 shows normalized bandgap movement at five different output power levels. The edge of the bandgap moves from ~1043nm to ~1035nm when the signal power increases from 0.5W to 157.1W (6dB power criteria), shown in Fig. 12. The measurement shows the guiding dynamics of the DMF1064 to change from leaky (at low power operation) closer to SM guiding (at high power operation). However, our observations in section 3 (signal core to cladding measurement) indicated that already above 80W of output power the DMF1064 guides at the SM region (increasing core to cladding ratio). This is caused by the gain dynamics, highest gain at the output end, and that the signal core to cladding ratio is effected more to the local bandgap position at the end of the rod fiber.

To obtain an estimate of the thermally induced refractive index change, a circular symmetric step-index fiber approximation to the DMF rod fiber was simulated by a beam propagation model, taking transverse hole-burning and the thermo-optical effect into consideration [8]. The core NA of 0.016 and core diameter of 60μm was chosen to match the MFD of the actual DMF fiber fundamental mode, and the Ytterbium concentration in the core was chosen to provide 27dB/m pump absorption at 976nm. The simulated rod fiber length was 1m and the seed level was constant at 1W. The pump power was altered in nine steps from 10W to 200W yielding signal levels from 6W to 153W. The boundary condition for the calculation of the thermal profile was chosen to be a Dirichlet boundary condition, in which the temperature at the fiber surface was fixed at room temperature.

Three examples of the thermally induced index profile are plotted on the same color scale for the change in refractive index from 0 to ~$1.5e^{-4}$ in Fig. 10 with signal power levels of (a) 38W, (b) 97W and (c) 153W. The largest change in refractive index occurs at the center of the

#160026 - $15.00 USD Received 14 Dec 2011; revised 16 Feb 2012; accepted 21 Feb 2012; published 24 Feb 2012

core and degrades as a function of radius. A change of the refractive index (Δn) at the end of the rod fiber is determined as the difference in the refractive index at $r = 0$ and $r = 54\mu m$ for $z = 1$ m. The first ring of resonators (DMF elements) are located at a mean radius of 54μm, which means that change of the refractive index is an approximation of the refractive index difference between the first ring of resonators and the center of the core. The change on the refractive index is only applied to the hexagonal core, shown in Fig. 11(a), as a step-index profile. The bandgap in the DMF rod fiber occurs because of the DMF elements, which implies that temperature difference between these elements and the core becomes the dominating reason for bandgap movement caused by the thermally induced refractive index change.

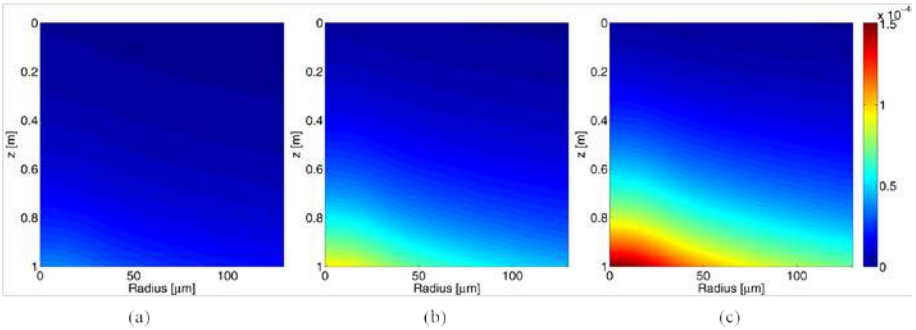

Fig. 10. The thermally induced refractive index profile of a circular symmetric fiber with similar properties as the DMF rod fiber used in the experiments with signal power level of (a) 38W, (b) 97W and (c) 153W.

Cross-sections of the DMF rod fiber were modeled numerically with the finite element method using the 'master' equation Eq. (1) and assuming harmonic modes for the z-component, where the thermally induced change in refractive index Δn was integrated.

$$\nabla \times \left[\frac{1}{\varepsilon_r(r)} \nabla \times \mathrm{H}(x, y) \right] = \left(\frac{\omega}{c} \right)^2 \mathrm{H}(x, y), \qquad (1)$$

The cross-section is symmetrical along the horizontal and vertical axis, and each subdomain is specified by setting the refractive index, shown in Fig. 11(a). The air cladding of the DMF rod fiber is represented by one outer ring having NA = 0.6 relative to silica level. From these simulations the core overlap of the FM as a function of wavelength was determined for Δn = 0 and for nine computed Δn obtained from the thermal simulations, shown in Fig. 11(b). The FM couples to the resonators inside the inner cladding structure when the wavelength decreases, thereby decreases the overlap in the core. However as the signal power level increases as a result of increasing pump power the position of the simulated bandgap edge is blue shifted similar to the experimental observed trend. This gives an estimate of the theoretical guiding regime of the DMF rod fiber.

#160026 - $15.00 USD Received 14 Dec 2011; revised 16 Feb 2012; accepted 21 Feb 2012; published 24 Feb 2012

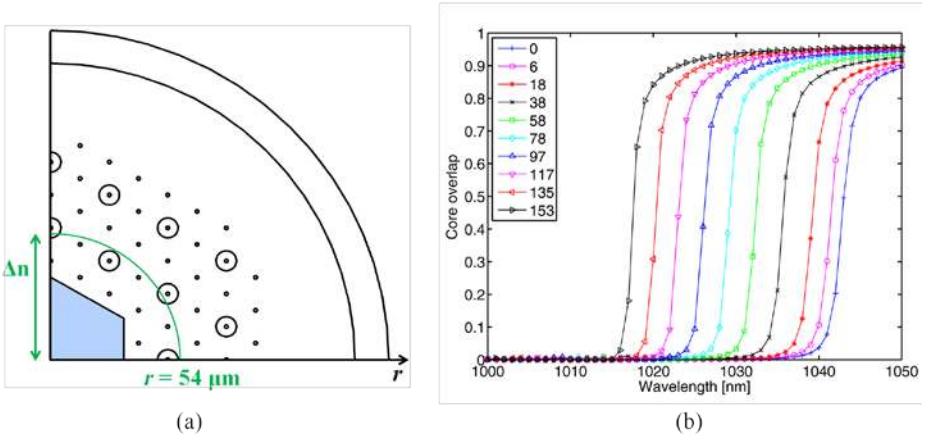

Fig. 11. (a) The modeled cross-section of the DMF rod fiber with indication of the zero level from the thermal simulations to estimate the Δn. (b) The fundamental mode bandgap edge movement as a function of wavelength for 10 different signal power levels.

The position of the bandgap edge is estimated as the wavelength, where the core overlap is reduced to 50%. This is shown in Fig. 12 together with the experimental estimation of the bandgap edge as a function of the output power level. For low output power levels the experimental and simulated position of the bandgap edge matches, but as the signal power level increases the simulated results estimate larger bandgap shift. The simulated badgap edge has a linear slope like the measured one. However, the measured bandgap edge has two points, at high output power levels, which are a bit off from the linear fit and this indicates saturation of the bandgap position. At the moment, we cannot explain the saturation effect of the bandgap edge position.

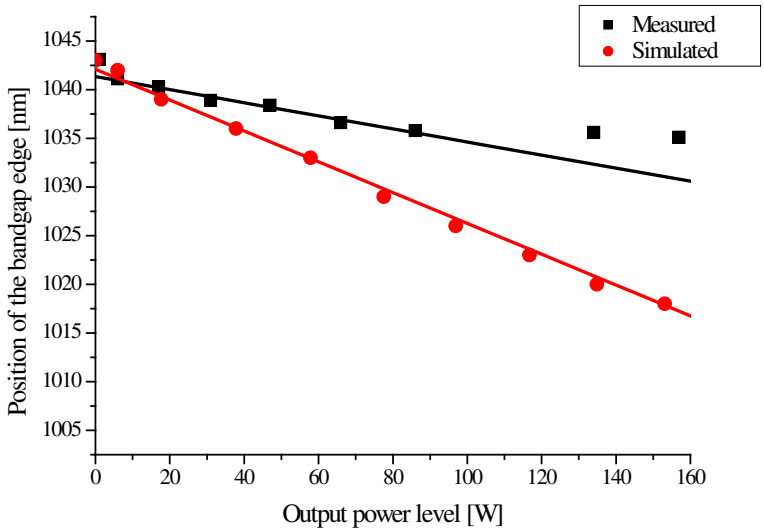

Fig. 12. Measured and simulated position of the bandgap edge with different output power levels.

The position of the simulated and measured bandgap edges exhibit different slopes because the simulations represent a local bandgap at the end of the rod fiber and the measurements an effective (average) bandgap over the whole length of the rod fiber. In

#160026 - $15.00 USD Received 14 Dec 2011; revised 16 Feb 2012; accepted 21 Feb 2012; published 24 Feb 2012

simulations, we use an increased homogeneous refractive index profile along the whole rod fiber length, for each output power level, but in the experiments the refractive index is decaying towards the input end, due to pump absorption.

Typically, measuring a core temperature of an active fiber or rod fiber is hard, or even impossible. A way to measure the temperature of the core would be vital when new high power fiber designs with extremely large effective areas are developed especially when higher and higher average power levels are required. As most of the fiber designs are made to support only one or few modes, even a small increase in the refractive index of the core will cause the fibers to support increasing number of modes and thereby decreasing the beam quality. Therefore, DMF rod fibers have a unique property where thermally induced refractive index change can be measured from the positions of the bandgap edge.

It has to be noted that even our experiments and simulations deviate as much as ~20nm at signal power level of ~150W still the order of magnitude is right. Both the experiments and simulations support the theory of thermally induced refractive index profile change inside the rod fiber. More trustful (simulated) thermal profile is achieved when the applied step-index model is modified to take account the full PCF structure including the air-cladding and non-perfectly matched boundary condition. Over estimation of the bandgap edge position at high signal power levels can be corrected using decaying refractive index profile along the rod fiber length, and including the full DMF structure in the simulation. In addition, we simulated the index difference between the core and the cladding and only changed the refractive index inside the hexagonal core, shown in Fig. 11(a), using a step-index like profile and the index of the cladding or the DMF elements is not changed. In reality the modes inside the core experience a thermally induced refractive index profile which has the maximum in the middle of the core and decreasing towards edge of the core.

Above mentioned improvements will of course increase the complexity of the model and increase the computation time significantly, but still they should be feasible to implement. We believe that enhanced simulations will decrease the deviation between the simulations and experiments and provide a great tool to further investigate the exact temperature and refractive index profile inside the DMF rod fibers.

5. Conclusion

In this paper, we have experimentally shown a rod fiber design with improved threshold-like onset of the mode instabilities utilizing a Distributed Mode Filtering (DMF) design in an amplifier configuration delivering up to 292W of average output power. We have demonstrated a power improvement of 44% before the onset level by operating the rod fiber in a leaky wavelength regime (at low power). In addition, we have studied the memory effect of threshold level of mode instabilities and demonstrated a photobleaching method recovering the fiber to its original state. The improved performance is discussed and explained by the guiding dynamics of the DMF rod fibers. The guiding dynamics are evaluated both by experiments and simulations. We measured a movement of the bandgap edge from 1043nm to 1035nm when the signal power level is increasing from 0.5W to 160W and show a new method to quantify the thermally induced change in the refractive index profile.

Acknowledgments

The project is supported with funding from the EU FP7 project LIFT (CP- IP 228587-1-LIFT) and The Danish Council for Independent Research and Technology and Production Sciences (FTP). The authors thank Dr. Jens Limpert and his group from Friedrich Schiller University Jena, Institute of Applied Physics for their collaboration and help.

#160026 - $15.00 USD Received 14 Dec 2011; revised 16 Feb 2012; accepted 21 Feb 2012; published 24 Feb 2012